

## Article

# Spectroscopic Identification of Amber Imitations: Different Pressure and Temperature Treatments of Copal Resins

Ting Zheng <sup>1</sup>, Haibo Li <sup>2,\*</sup>, Taijin Lu <sup>2</sup>, Xiaoming Chen <sup>1</sup>, Bowen Li <sup>1</sup> and Yingying Liu <sup>3</sup>

<sup>1</sup> Beijing Laboratory, National Gemstone Testing Center, Beijing 100013, China; zhting1990@gmail.com (T.Z.); chenxm141@163.com (X.C.); bowen\_li\_817@163.com (B.L.)

<sup>2</sup> National Gems & Jewelry Technology Administrative Center, Beijing 100013, China; taijinlu@hotmail.com

<sup>3</sup> Century Amber Museum, Shenzhen 518101, China; liuyingying611@hotmail.com

\* Correspondence: lihb@ngtc.com.cn; Tel.: +86-010-58276143

**Abstract:** Copal resins can be treated with heat and/or pressure to imitate ambers in the gem market. To explore the effects of different modification conditions on post-treatment spectral changes, five experimental methods with different temperature–pressure parameters were designed to modify two types of copal resins. The treated copal resins were examined by infrared, Raman and nuclear magnetic resonance spectroscopy. Results indicate that all the treatment methods simulate the maturation process, with spectral characteristics becoming more similar to those of ambers. Multi-stage heat–pressure treatment has the most significant effect on Colombia and Madagascar copal resins, with their spectra being similar to those of Dominican and Mexican ambers. Rapid high-temperature treatment at 180 °C modified the Borneo copal resin, with its infrared spectrum developing a “Baltic shoulder” resembling that of heat-treated Baltic amber. Even though there are many similarities between treated copal resins and natural ambers, they can still be distinguished by spectroscopic methods.



**Citation:** Zheng, T.; Li, H.; Lu, T.; Chen, X.; Li, B.; Liu, Y. Spectroscopic Identification of Amber Imitations: Different Pressure and Temperature Treatments of Copal Resins. *Crystals* **2021**, *11*, 1223. <https://doi.org/10.3390/cryst11101223>

Academic Editor: José L. Arias

Received: 6 September 2021

Accepted: 5 October 2021

Published: 11 October 2021

**Publisher's Note:** MDPI stays neutral with regard to jurisdictional claims in published maps and institutional affiliations.



**Copyright:** © 2021 by the authors. Licensee MDPI, Basel, Switzerland. This article is an open access article distributed under the terms and conditions of the Creative Commons Attribution (CC BY) license (<https://creativecommons.org/licenses/by/4.0/>).

**Keywords:** Colombia copal resin; Madagascar copal resin; Borneo copal resin; amber; FTIR spectrum; Raman spectrum; <sup>13</sup>C NMR spectrum

## 1. Introduction

Amber forms when resin from certain trees hardens and gradually fossilizes over time. Polymerization of organic hydrocarbon molecules first transforms the resin into copal resin, which then undergoes further devolatilization and fossilization (due mainly to cross-linkage between hydrocarbon chains) during burial in sediments to become amber [1–5]. Copal resin is thus a subfossil resin at an intermediate stage between resin and amber, bearing a high degree of similarity in appearance, physical properties and chemical composition to amber. The process of turning copal resin into amber requires around 13 Myr [6]. Based on this vague definition, Solórzano-Kraemer et al. [7] proposed that natural tree resin from Borneo (Southeast Asia, especially from islands of the Indo-Australian Archipelago) should be classified as copal resin, with geological ages of 3–12 Myr. Other examples are the Colombia and Madagascar copal resins that formed several hundred to ~10,000 years ago, according to <sup>14</sup>C dating [7–9].

It is well known that as tree resins lose volatile substances, monomers combine to form more complicated structures in the maturation process during fossilization. Maturation is enhanced when the resin is buried in an environment with elevated pressure and temperature. With the rapid development of the gem market, treatment of copal resin with artificial heat and pressure is a popular means of accelerating the fossilization process so that “ambers” can be produced within even a few days [1]. Wang et al. [10] described processing methods commonly used with amber products in the gem market, including pressure, temperature, atmosphere and other parameters. The modification of copal resins may involve any such methods, but few data are available concerning specific

processes [11,12]. Abduriyim et al. [1] proposed a two-stage autoclave method with different combinations of pressure and temperature, with such treatment artificially aging copal resins. However, it remains unclear as to what the optimum temperature–pressure parameters are for the fossilization process, and whether there exist universally optimized parameters for all types of copal resin.

Here we consider “maturity” in terms of changes in the structure and composition of copal resins, reflecting both age and evolutionary history (whether artificial or natural) [13]. Low-maturity copal resin contains more unsaturated components than amber, and the laboratory analysis of unsaturated components is an important means for distinguishing between amber and copal resin. In our experiments we adjusted temperature–pressure conditions to accelerate the maturation of copal resin.

Based on their spectral characteristics and botanical sources, copal resins are here divided roughly into two types, as follows. Type (1) encompasses copal resins from Colombia and Madagascar, which contain a number of unsaturated components (terpenes) with three characteristic infrared (IR) absorption bands near 3078, 1642 and 888  $\text{cm}^{-1}$ . These resins are presumed to have been produced by *Hymenaea* species, based on chemical analysis and surveys of the major resin-producing trees of Colombia and Madagascar [9,13–16]. They have remarkably consistent characteristics in their IR, Raman and NMR spectra. Type (2) comprises Borneo copal resin, which contains fewer unsaturated components. The IR spectra for this type lack peaks at 3078 and 1642  $\text{cm}^{-1}$  and the absorption intensity at 888  $\text{cm}^{-1}$  is weak, making its spectral characteristics significantly different from that of type (1). Its origin has been linked to the *Dipterocarpaceae* family [8,13].

To date, there have been few reports of successful modification of Borneo copal resins. Considering the large-scale production of copal resin or amber processing technology, we attempted to establish the most suitable modification conditions for Colombia, Madagascar and Borneo copal resins, exploring surface and internal changes, and studying differences between treated products and ambers and the effects of specific temperature–pressure conditions.

## 2. Materials and Methods

### 2.1. Samples

A total of 65 copal resins from Colombia (13), Madagascar (26) and Borneo (26) were selected from a collection of resins and ambers at the National Gemstone Testing Center (Beijing, China). In this case, 47 typical samples from these three sets were cut into three or six portions of which two or five, respectively, were used in modification experiments under different temperature, pressure and atmospheric conditions, with the remaining portion being retained as untreated for comparison.

### 2.2. Temperature–Pressure Conditions

Equipment used in the experiments is shown in Figure 1, and the specific experimental parameters in Table 1. Based on their characteristics, five different methods were applied in modifying the resin samples (Table 1).

These five experiments can be divided into two categories; two of the five are heat-only treatments and the other three are heat–pressure treatments, which are conducted under pressurized conditions. Specifically, the two heat treatments included slow low-temperature and rapid high-temperature treatments. The former involved heating samples at 90 °C for 90 days under ambient pressure; the latter involved heating at 100 °C, 120 °C, 140 °C, 160 °C or 180 °C for 1 day, again under ambient pressure. No vacuum was applied in these two heat treatment methods. The three pressurized experiments, including two single-stage heat–pressure treatments and one multi-stage heat–pressure treatment, were undertaken under vacuum and in a nitrogen-filled environment, with ventilation of nitrogen carried out once a day during the process.

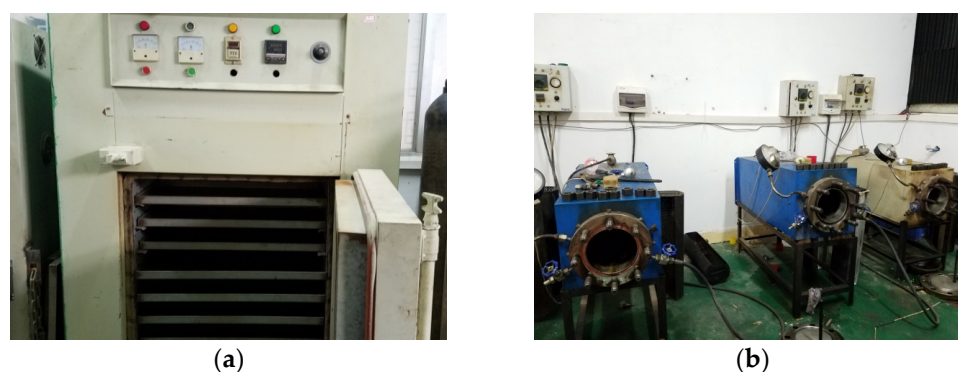


**Figure 1.** Experimental equipment: (a) heat treatment equipment with temperature and time controls; (b) heat–pressure treatment equipment with temperature, pressure and time controls.

**Table 1.** Experimental parameters and copal resin samples of different origins treated by different methods.

Characteristics	Heat Treatments			Heat–Pressure Treatments		
	Slow Low-Temperature Treatment	Rapid High-Temperature Treatment	Single-Stage Heat–Pressure Treatment (140/25)	Single-Stage Heat–Pressure Treatment (180/35)	Multi-Stage Heat–Pressure Treatment	
Sample preparation	Cut into 3 pieces	Cut into 6 pieces	Cut into 3 pieces	Cut into 3 pieces	Cut into 3 pieces	
Temperature (°C)	90	100/120/140/160/180	140	180	–	
Pressure (bar)	(atmospheric)	(atmospheric)	25	35	–	
Heating time (days)	90	1	7	7	–	
Ventilation of N <sub>2</sub>	–	–	once a day	once a day	–	
Samples from Colombia	Col-009 *	Col-005 Col-013 *	–	–	Col-003 Col-004 Col-006 *	Col-007 Col-008 Col-010
Samples from Madagascar	Ma-002 Ma-009 Ma-013 Ma-014 *	Ma-005 * Ma-025	Ma-003 Ma-011 Ma-016 Ma-019	Ma-007 Ma-010 Ma-012 Ma-020	Ma-004 * Ma-006 Ma-008	Ma-015 Ma-017 Ma-018
Samples from Borneo	Bor-001 Bor-002 * Bo-007 Bor-019	Bor-024 Bor-026 *	Bor-003 Bor-004 Bor-005 Bor-006	Bor-011 Bor-013 Bor-015 Bor-017	Bor-008 Bor-009 Bor-010 * Bor-012	

\* Samples tested by <sup>13</sup>C NMR spectroscopy.

The two single-stage heat–pressure treatments were undertaken at 140 °C–25 bar and 180 °C–35 bar (abbreviated hereinafter as 140/25 and 180/35), both lasting 7 days. For multi-stage heat–pressure treatment, temperature and pressure were gradually increased in a certain environment for a period of time, then reduced slowly to ambient conditions, with this cycle being repeated several times. Procedural details are confidential due to processing factory requirements, but the conditions resemble those used in the study of “green amber” by Abduriyim et al. [1].

### 2.3. Analytical Methods

#### 2.3.1. Fourier Transform Infrared Spectroscopy

The facilities of the National Gemstone Testing Center were used for Fourier transform IR (FTIR) spectroscopic analysis of copal resins and ambers, using a Thermo Scientific Nicolet iN10 spectrometer (Waltham, MA, USA) and an OMNIC Picta workstation (Waltham, MA, USA). A sampling-kit diamond cell was used to compress sample powder into thin

films to achieve an optical path suitable for transmission measurements and spectra were acquired with 128 scans over 600–4000  $\text{cm}^{-1}$  with a resolution of 4  $\text{cm}^{-1}$ . A Thermo Scientific Nicolet 6700 FTIR spectrometer (Waltham, MA, USA) was used to acquire reflectance spectra by K–K transformation, with 64 scans over 400–4000  $\text{cm}^{-1}$  with a resolution of 4  $\text{cm}^{-1}$ . All data were analyzed by OMNIC software (Waltham, MA, USA) with spectra being normalized with respect to the most intense band in the range.

### 2.3.2. Raman Spectroscopy

Sample Raman spectra were obtained using a Renishaw (England) inVia Reflex micro-Raman spectrometer with 785 nm excitation, a scanning range of 4000–100  $\text{cm}^{-1}$  and resolution of 1  $\text{cm}^{-1}$ . Three spectral accumulations were necessary, each of ~10 s exposure, to achieve spectra of the desired quality with a nominal laser power of 250 mW. Fluorescence backgrounds were subtracted from the spectra, which were again normalized to improve comparison of intensities.

### 2.3.3. Nuclear Magnetic Resonance Spectroscopy

A Bruker (Germany) Ascend™ 400WB nuclear magnetic resonance (NMR) spectrometer, at the Beijing University of Chemical Technology, Beijing, China, was used for solid-state  $^{13}\text{C}$  NMR spectroscopic analyses of 9 typical samples (Table 1). Each sample of >100 mg was powdered in a mortar for the  $^{13}\text{C}$  analyses. Spectra were collected by using a 4 mm MAS probe with a proton frequency of 400.13 MHz.  $^{13}\text{C}$  spectra at 100.6 MHz of the solid samples were acquired under the following parameters: 38ms acquisition time, a time domain of 3k points, a spectral width of 41 kHz, 800 scans, an FID resolution of 13 Hz, a dwell time of 12.3  $\mu\text{s}$  and a pre-scan delay of 8.6  $\mu\text{s}$ .

## 3. Results and Discussion

Colombia and Madagascar copal resins were classified as one group, and Borneo samples as another. Copal samples within a group exhibited identical or similar changes under changing treatment conditions.

During treatment, the colors of samples were darkened to varying degrees, developing a brown hue, with the surface of some samples appearing melted and cracked (Figure 2), especially for the Borneo resins, while their fluorescence changed to a whitish blue or a chalky, earthy yellow.

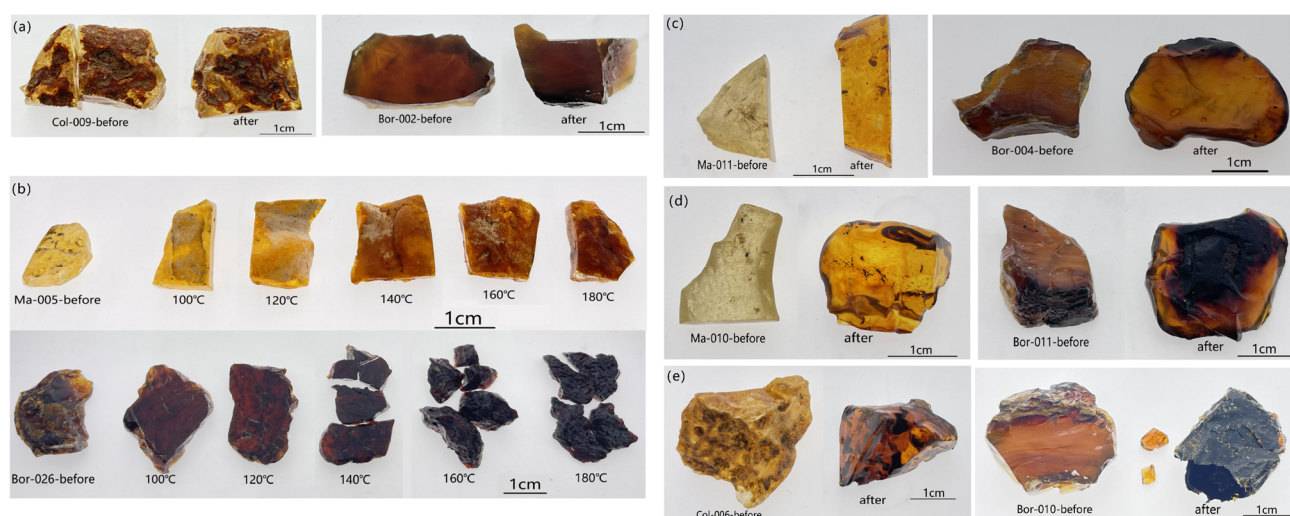


**Figure 2.** Representative samples used for the experiments: (a) slow low-temperature treatment; (b) rapid high-temperature treatment; (c) single-stage heat–pressure treatment (140/25); (d) single-stage heat–pressure treatment (180/35); (e) multi-stage heat–pressure treatment. For each sample, the untreated portion is shown on the left, and the treated portion on the right. For samples Ma-005 and Bor-026, the heating temperature is also indicated.

### 3.1. Colombia and Madagascar Copal Resins

#### 3.1.1. FTIR Spectroscopy

The IR spectra of Colombia and Madagascar copal resins are highly consistent, with their IR band shapes being very similar with only slight variations in some specific peak positions and relative intensities. For convenience, we use the same wavenumber to describe the same IR feature appearing in approximately the same positions in different spectra, as for Raman spectra. Most visible features of copal resin spectra have been reported previously [1,3,5,17–19], including the IR absorption band at  $\sim 3078\text{ cm}^{-1}$  assigned to the C–H stretching vibration of the exocyclic C=CH<sub>2</sub> group, which is barely detectable in ambers. Strong absorption bands at 2930, 2867 and  $2850\text{ cm}^{-1}$  are attributed to the C–H stretching vibration. The  $1697\text{ cm}^{-1}$  band is due to C=O stretching and the  $1642\text{ cm}^{-1}$  band to exocyclic non-conjugated C=C stretching. We also detected 1444 and  $1385\text{ cm}^{-1}$  features related to the CH<sub>2</sub>–CH<sub>3</sub> bending vibration; and 1262, 1175 and  $1040\text{ cm}^{-1}$  features of the C–O stretching vibration. The sharp peak at  $888\text{ cm}^{-1}$ , assigned to out-of-plane C–H bending in an exocyclic methylene bond, was always evident.

In both the slow low-temperature (e.g., Col-009, Figure 3a) and rapid high-temperature treatments (e.g., Ma-005, Figure 3b), the IR spectra of Colombia and Madagascar copal resins displayed a gradual shift in the strong absorption peak near  $1697\text{ cm}^{-1}$  with increasing temperature or heating time, to  $\sim 1712\text{ cm}^{-1}$ , while the 3078, 1642 and  $888\text{ cm}^{-1}$  bands became weaker.

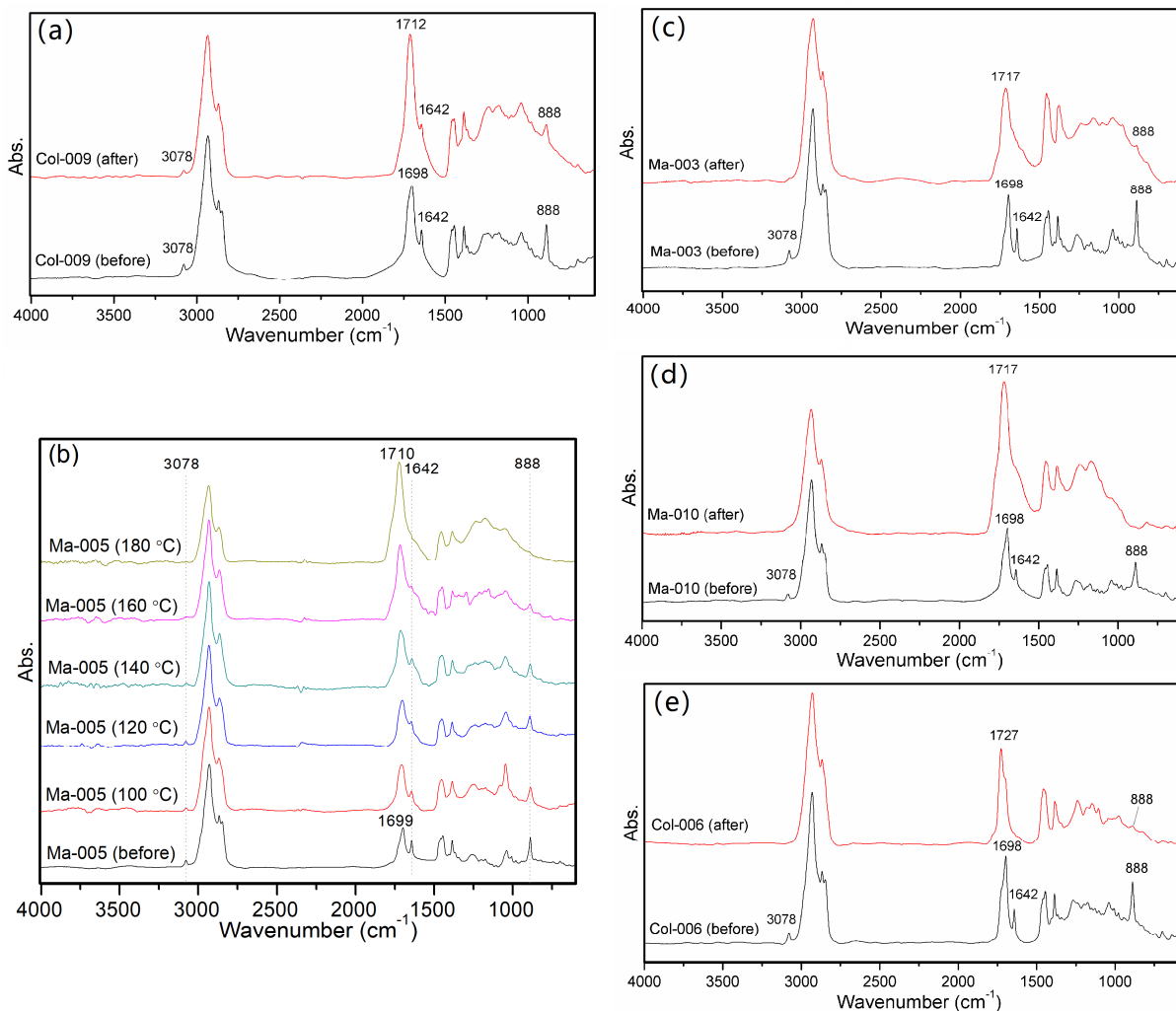


**Figure 3.** IR spectra of Colombia and Madagascar samples before and after treatment: (a) slow low-temperature treatment; (b) rapid high-temperature treatment; (c) single-stage heat–pressure treatment (140/25); (d) single-stage heat–pressure treatment (180/35); (e) multi-stage heat–pressure treatment.

During the single-stage heat–pressure treatment (140/25) (e.g., Ma-003, Figure 3c), single-stage heat–pressure treatment (180/35) (e.g., Ma-010, Figure 3d) and multi-stage heat–pressure treatment (e.g., Col-006, Figure 3e), spectral changes in Colombia and Madagascar samples were similar, with differences appearing mainly in specific peak positions and relative intensities (Table 2). The spectra of all copal samples display significant changes after three heat–pressure treatments. The strong absorption peak near  $1697\text{ cm}^{-1}$  shifts gradually to  $1717$  or  $1727\text{ cm}^{-1}$ , and the three characteristic bands diminish or disappear completely. The absorption at approximately  $1259\text{ cm}^{-1}$  shifts to  $1242\text{ cm}^{-1}$  in the C single-bond region.

**Table 2.** Changes in IR spectra of Colombia and Madagascar copal resin during treatment.

Sample	Modification Method	Changes in IR Spectra			
		Before Treatment		After Treatment	
		C=O Related to Esters ( $\text{cm}^{-1}$ )	Absorption of 3078, 1642, 888 $\text{cm}^{-1}$	C=O Related to Esters ( $\text{cm}^{-1}$ )	Absorption of 3078, 1642 and 888 $\text{cm}^{-1}$
Col-009	Slow low-temperature treatment	1697	strong	1712	moderate
Ma-005	Rapid high-temperature treatment	1697	super strong	100 °C	strong
				120 °C	strong
				140 °C	moderate
				160 °C	moderate
				180 °C	very weak
Ma-003	Single-stage heat–pressure treatment (140/25)	1697	strong	1717	Peaks at 3078 and 1642 $\text{cm}^{-1}$ disappeared, weak peak at 888 $\text{cm}^{-1}$
Ma-010	Single-stage heat–pressure treatment (180/35)	1697	strong	1717	Peaks at 3078, 1642 and 888 $\text{cm}^{-1}$ disappeared
Col-006	Multi-stage heat–pressure treatment	1697	strong	1727	Peaks at 3078 and 1642 $\text{cm}^{-1}$ disappeared, very weak peak at 888 $\text{cm}^{-1}$

As copal resin is less mature than amber, its content of labdanoid diterpene monomer (which is not involved in polymerization) is higher. As maturity increases during treatment, the exocyclic unsaturated bonds are gradually broken and the relative intensities of their absorption peaks reduced until they disappear. Peak intensity changes thus reflect the effects of different processing methods.

### 3.1.2. Raman Spectroscopy

The quality of Raman spectra of copal resins depends on laser power and sample conditions. High-energy lasers used in Raman spectroscopy may cause thermal alteration, with strong fluorescence of organic samples. Amber and copal resin with a high degree of aging or oxidation are more likely to produce a strong fluorescence background. Here we used 785 nm excitation, but Raman peaks were sometimes not evident, especially with Borneo copal resins.

Copal resins, both natural and artificially modified, have Raman spectra characteristic of their origins, botanical sources, maturity and thermal history. Raman shifts in spectra of copal resins are listed in Table 3.

**Table 3.** Assignment of Raman shifts in spectra of copal resins of different origin.

Colombia	Madagascar	Borneo	Assignment [18,20–24]
3078	3080		$\nu(\text{CH}) \text{ C}=\text{CH}_2$
2986	2984		$\nu(\text{CH}_2)$
2926	2926	2926	$\nu(\text{CH}_2)$
2893	2889	2908	$\nu(\text{CH}_2)$
2865	2867	2869	$\nu(\text{CH}_2)$
2845	2848		$\nu(\text{CH}_2)$
		1708	$\nu(\text{C}=\text{O})$
		1672	
		1655	$\nu(\text{C}=\text{C})$ trans conjugated
1642	1643		$\nu(\text{C}=\text{C})$ non-conjugated
1470	1470		$\delta(\text{CH}_2), \delta(\text{CH}_3)$
1440	1440	1443	$\delta(\text{CH}_2), \delta(\text{CH}_3)$
1408	1408		$\delta(\text{CH}_2), \delta(\text{CH}_3)$
1386	1383		$\delta(\text{CH}_2), \delta(\text{CH}_3)$
1361	1361	1368	$\delta(\text{CH}_2), \delta(\text{CH}_3)$
1328	1330		$\delta(\text{CH}_2), \delta(\text{CH}_3)$
		1317	$\delta(\text{CH}_2), \delta(\text{CH}_3)$
1309	1309		$\delta(\text{CH}_2), \delta(\text{CH}_3)$
1283	1284		
		1260	
1243	1244	1237	
1200	1200		$\delta(\text{CCH}), \delta(\text{C}-\text{O})$
1133	1133		$\nu(\text{CC})$ ring breathing, $\delta(\text{C}-\text{O})$
		1127	
1108	1109		$\nu(\text{C}-\text{C})$
1079	1079	1084	
1056	1056	1061	
		1043	
1007	1006		
		1002	$\nu(\text{CC})$ aromatic
979	980		$\rho(\text{CH}_2), \rho(\text{CH}_3)$
		956	
946	946		
935	936		$\rho(\text{CH}_2), \rho(\text{CH}_3), \nu(\text{CC})$
885	886	885	$\rho(\text{CH}_2)$ of $\text{C}=\text{C}$ double bonds
859	860		
821	821	823	
		801	aromatic hydrocarbon deformation
745	745		$\nu(\text{CC})$ isolated
		734	$\nu(\text{CC})$ isolated
697	697		
		680	
642	641		
600	600		
577	577		
554	554	552	$\delta(\text{CCO}), \delta(\text{COC})$ in-plane deformation
529	529		
491	491		
		464	

As previously reported [18,20–24], apart from a weak band at  $3078 \text{ cm}^{-1}$ , the wavelength range of  $2700\text{--}3100 \text{ cm}^{-1}$  represents the stretching vibration of the saturated  $\text{C}-\text{H}$  bond, with its corresponding bending regions being near  $1470\text{--}1300$  and  $980\text{--}880 \text{ cm}^{-1}$ , including a strong peak at  $1440 \text{ cm}^{-1}$ . Peaks at  $1655$  and  $1642 \text{ cm}^{-1}$  are attributed to  $\text{C}=\text{C}$  double-bond stretching.  $\text{C}-\text{C}$  and  $\text{C}-\text{O}$  stretching vibrations appear in the range of  $1125\text{--}1000 \text{ cm}^{-1}$ . The deformation bands of aromatic compounds and the  $\text{C}-\text{O}-\text{C}$  stretching band of cyclic ethers (and polysaccharides) are in the range of  $950\text{--}800 \text{ cm}^{-1}$ , with a weak

feature at  $888\text{ cm}^{-1}$ . Bands below  $800\text{ cm}^{-1}$  are due to out-of-plane deformation vibration of aromatic compounds, with C–C, C–O and C–O–C vibrations below  $550\text{ cm}^{-1}$ .

Raman shifts of Colombia and Madagascar copal resins are concentrated in three regions:  $3100\text{--}2700$ ,  $1642$  and  $1440\text{ cm}^{-1}$ , with characteristic peaks near  $3078$ ,  $1642$  and  $888\text{ cm}^{-1}$ , consistent with the IR spectrum.

Previous studies [18,21] have shown that the decrease in band intensity at  $1640\text{ cm}^{-1}$  relative to  $1440\text{ cm}^{-1}$  provides a measure of maturity of natural resins, with maturation and other oxidative processes leading to the elimination of C=C double bonds in natural resins and enhancing monomer cross-linking. However, a later study [23] found that the peak-height ratio at  $1640$  and  $1440\text{ cm}^{-1}$  ( $H^{1640}/H^{1440}$ ) cannot be linked to sample maturity, with even the same sample displaying variable maturity based on  $H^{1640}/H^{1440}$  ratios at different positions. For this study, however, it still has application in comparison of maturities of samples before and after modification.

For Colombia and Madagascar copal resins, all treatment methods resulted in an increase in the fluorescence background, with weak Raman shifts near  $3078$  and  $888\text{ cm}^{-1}$  weakening or disappearing and with reduced  $H^{1640}/H^{1440}$  ratios, suggesting the breaking of C=C double bonds with increasing maturity. Taking sample Col-006 processed by multi-stage heat–pressure treatment as an example,  $H^{1640}/H^{1440}$  reduced from  $1.44$  to  $0.84$ , a decrease of  $42\%$ .

To summarize, the three heat–pressure treatments (e.g., Ma-011, Ma-010 and Col-006, Figure 4) changed Raman spectra more remarkably than did the two heat treatments (e.g., Col-009 and Ma-005, Figure 4) applied to Colombia and Madagascar copal resins. Reductions in  $H^{1640}/H^{1440}$  ratios during heat treatments were generally in the range of  $7\text{--}14\%$ , and those of heat–pressure treatments were  $14\text{--}42\%$  (Table 4). The decrease in  $H^{1640}/H^{1440}$  ratio can be used as a quantitative indicator of the modification effect of treatment.

### 3.1.3. NMR Spectroscopy

The  $^{13}\text{C}$  NMR spectra of amber and copal resin comprise four major regions [3,25–27]: (1)  $10\text{--}60$  ppm is a region of resonances of saturated carbons, includes methyl ( $-\text{CH}_3$ ), methylene ( $-\text{CH}_2-$ ),  $-\text{CH}_2\text{OH}$  and  $-\text{CHOH}$  groups; (2)  $60\text{--}90$  ppm is the characteristic region indicating chemical shifts in aliphatic O–C functional groups; (3)  $100\text{--}150$  ppm is the resonance signal region which includes unsaturated carbons such as olefins, cycloolefins and aromatics; (4)  $160\text{--}220$  ppm is the functional group region of carbonyl carbons, including weak resonance signals of carbonyl carbons in esters, acids or (COO $-$ ) carboxylate.

Table 5 shows  $^{13}\text{C}$  NMR band assignments for copal resins from different origins. NMR resonance peaks in the unsaturated carbon region are of great significance in indicating resin maturity. In the double-bonded carbon region at  $100\text{--}150$  ppm, four carbon signals were detected near  $148$ ,  $139$ ,  $125$  and  $107$  ppm in the spectra of Colombia and Madagascar copal resins. Singly substituted alkene carbons (C–HC=CH–C), as found in straight chains or within rings, resonate at  $125$  and  $139$  ppm while unsubstituted alkene carbons (C=CH $_2$ ) resonate at  $107$  ppm and disubstituted alkene carbons ( $>\text{C}=\text{C}$ ) near  $148$  ppm [6,15,28]. An exomethylene or terminal group thus has resonances at both  $107$  and  $148$  ppm, with both showing the presence of a large number of unsaturated components (terpenes).

Whether treated by slow low-temperature treatment (e.g., Ma-014, Figure 5a) or rapid high-temperature treatment (e.g., Col-013, Figure 5a), the  $^{13}\text{C}$  NMR spectra of Colombia and Madagascar copal resin samples displayed little change, although they did change significantly after multi-stage heat–pressure treatment (e.g., Col-006 and Ma-004, Figure 5a). The resonance peaks at  $107$  ppm and  $148$  ppm became much weaker, indicating that the treatment simulates the process of maturation to a considerable extent. The intensities of exocyclic methylene carbon signals resolved at  $107$  and  $148$  ppm decreased with increasing maturity, possibly owing to intermolecular cross-linkage of exocyclic methylene groups.



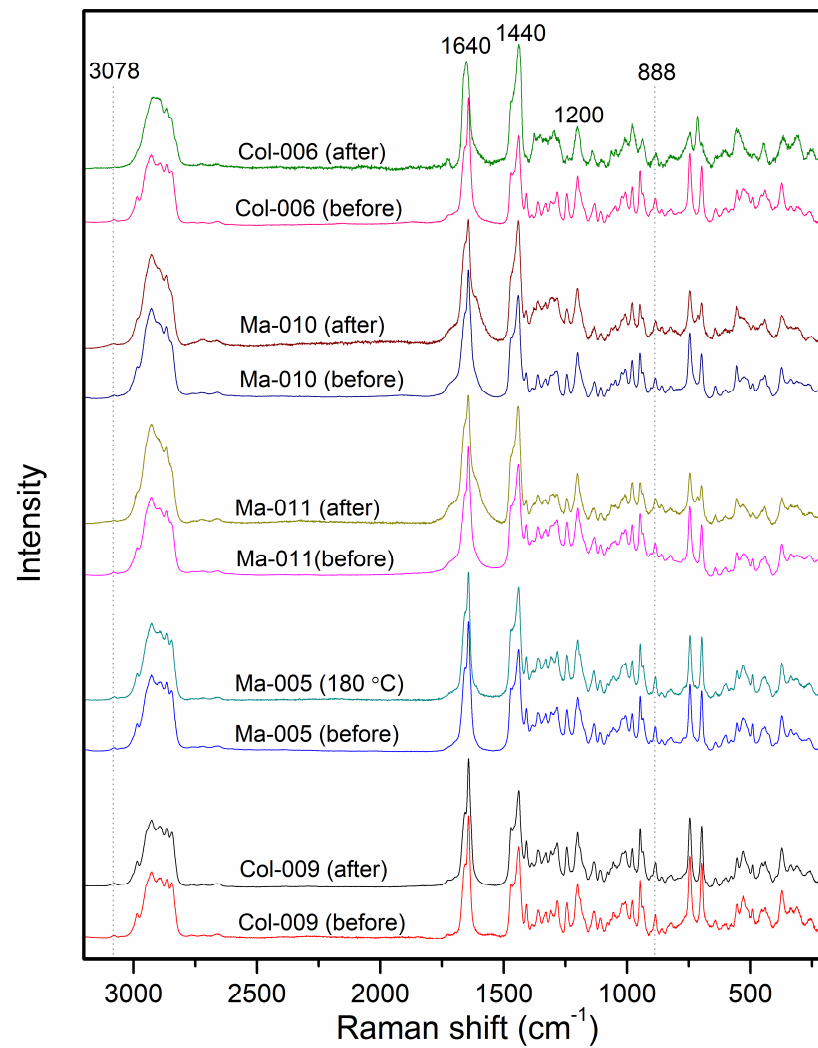


**Figure 4.** Raman spectra of Colombia and Madagascar resins before and after treatment (fluorescence background subtracted). From bottom to top: slow low-temperature treatment (Col-009), rapid high-temperature treatment (Ma-005), single-stage heat–pressure treatment (140/25) (Ma-011), single-stage heat–pressure treatment (180/35) (Ma-010) and multi-stage heat–pressure treatment (Col-006).

**Table 4.** Changes in  $H^{1640}/H^{1440}$  ratios of samples during treatment.

Sample Number	$H^{1640}/H^{1440}$ (Before)	$H^{1640}/H^{1440}$ (After)	Decrease in Ratio (%)	Sample Number	$H^{1640}/H^{1440}$ (Before)	$H^{1640}/H^{1440}$ (After)	Decrease in Ratio (%)
Col-009	1.52	1.41	7.3	Bor-002	0.67	—*	—
Col-006	1.44	0.84	42	Bor-026	—*	—*	—
Ma-014	1.47	1.36	7.5	Bor-005	0.58	—*	—
Ma-005	1.46	1.25	14	Bor-015	0.73	—*	—
Ma-004	1.44	0.83	42	Bor-010	0.52	—*	—
Ma-010	1.31	1.13	14	Bor-002	0.67	—*	—
Ma-011	1.37	1.12	18	Bor-026	—*	—*	—

\* Unable to calculate  $H^{1640}/H^{1440}$  ratio because the fluorescence background was too strong.

**Table 5.** Assignment of  $^{13}\text{C}$  NMR spectral bands of copal resins of different origin.

Chemical Shift Range (ppm)	Assignment [2,3,25–27]	Colombia (Represented by Col-006)	Madagascar (Represented by Ma-004)	Borneo (Represented by Bor-002)
14–18	C–C single bond (primary carbon)	15.68	15.54	16.21
19–21	C–C single bond (methyl in the ring)	19.01	19.02	21.83
22–36	C–C single bond (secondary carbon)	24.64	24.62	26.71
		27.10	26.92	—
		33.84	33.68	36.87
37–50	C–C single bond (quaternary carbon)	38.77	38.42	—
		47.86	47.71	48.04
		49.82	49.86	—
51–60	C–O single bond (tertiary carbon)	52.87	52.43	—
		57.32	57.46	—
61–75	C–O single bond (quaternary and tertiary carbon)	70.91	71.99	—
76–90	C–O single bond (quaternary carbon)	—	—	—
91–110	C=C double bonds (alkene)	107.07	106.71	—
111–130	C=C double bonds (aromatic)	125.56	124.65	125.60
131–139	C=C double bonds (heterocyclic aromatic)	138.92	139.41	134.46
140–150	C=C double bonds (substituted aromatic carbon)	147.90	147.97	—
165–178	C=O double bond (carboxylic acids, esters)	—	—	—
179–220	C=O double bonds (Ketones, aldehydes)	182.52	182.30	—
		186.10	186.02	—

Comparison of the NMR spectra of ambers and copal resins of different origins indicates that the resonance peak at 14–18 ppm in the saturated region, due to C–C single bonds (primary carbon) of adeps-methyl groups [3,25], appears only with copal resins. This is assumed to be an NMR typical peak of immature resins, which may shift to a higher field with increasing age until the C–C bond is broken. For example, the resonance near 16 ppm disappeared after multi-stage heat–pressure treatment (e.g., Col-006 and Ma-004, Figure 5a).

### 3.1.4. Comparison of Copal and Amber Spectra

Comparison of all spectral data for Colombia and Madagascar copal resins that underwent the five types of treatment methods detailed above indicates that the effects of three heat–pressure treatments are more significant than those of two heat treatments. The 3078, 1642 and 888  $\text{cm}^{-1}$  peaks, which characterize copal resins, became obviously weaker or even disappeared during treatment in both IR and Raman spectra.

Comparison of the three types of heat–pressure treatment indicates that multi-stage heat–pressure treatment has the most evident modification effect. The characteristic IR absorption bands at 3078, 1642 and 888  $\text{cm}^{-1}$  did not disappear completely, but the overall pattern of the copal spectra closely resembled those of ambers from Dominica and Mexico (Figure 6). In addition, resonance peaks at 107 and 148 ppm were obviously weakened.

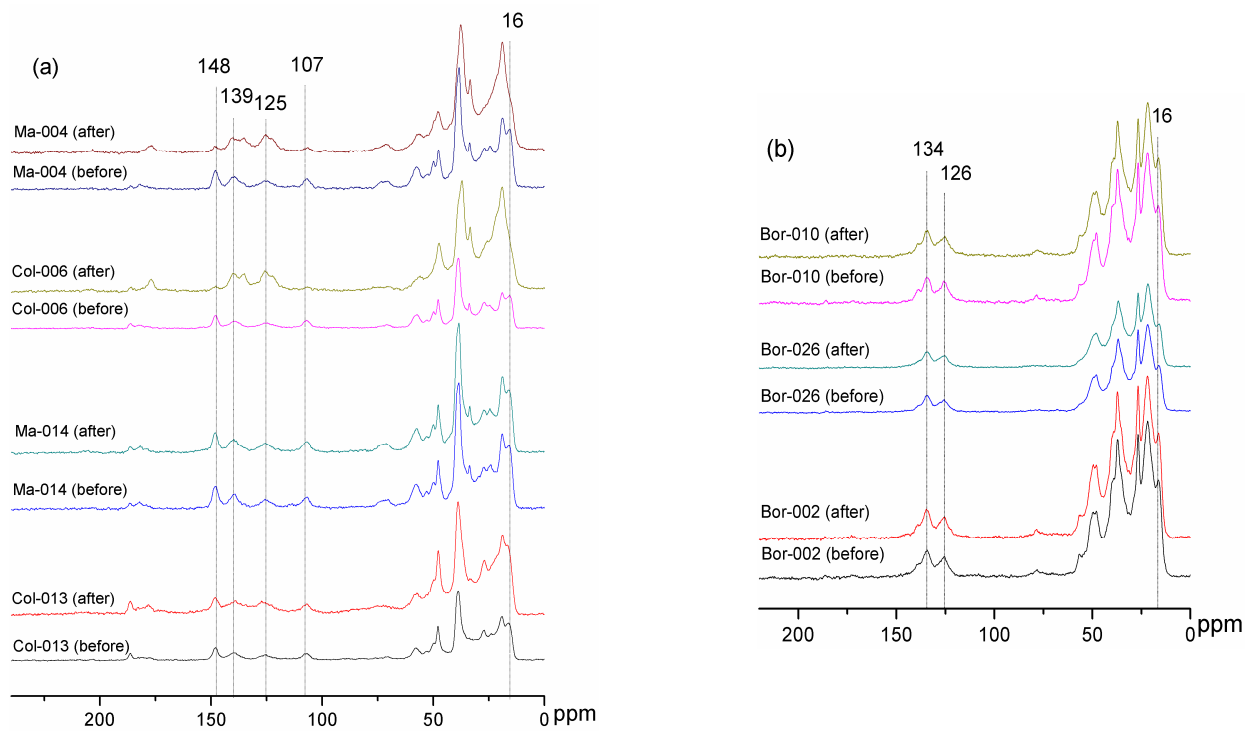


**Figure 5.**  $^{13}\text{C}$  NMR spectra of copal resins before and after treatment: (a) Colombia and Madagascar samples; (b) Borneo samples.

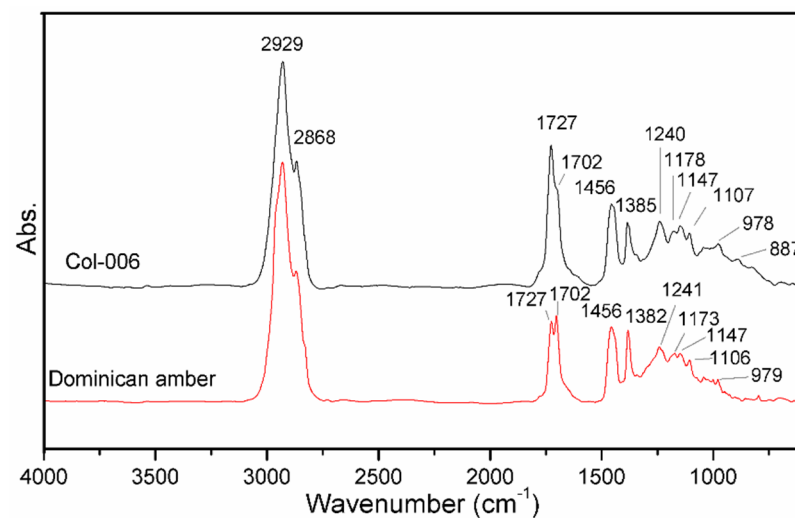


**Figure 6.** IR spectra of Dominican amber and sample Col-006 after multi-stage heat-pressure treatment.

The IR spectra of treated copal resin are similar to those of amber but can still be recognized as being copal resin. Sample Col-006, for example, which underwent multi-stage heat-pressure treatment, was sampled at three different depths in the same position for IR spectroscopic analysis. As sampling depth increased, characteristic bands at 3078, 1642 and  $888\text{ cm}^{-1}$  began to reappear with increasing intensity (Figure 7). This indicates that, although such modification treatment enhanced the maturity of copal resin, it did not completely fossilize the resin to amber, which required millions of years of geological processes. The exterior may look similar to amber, but the interior retains characteristics of copal resin. If a sample cannot be fully confirmed by this method, its identification can be assisted by NMR spectroscopy.

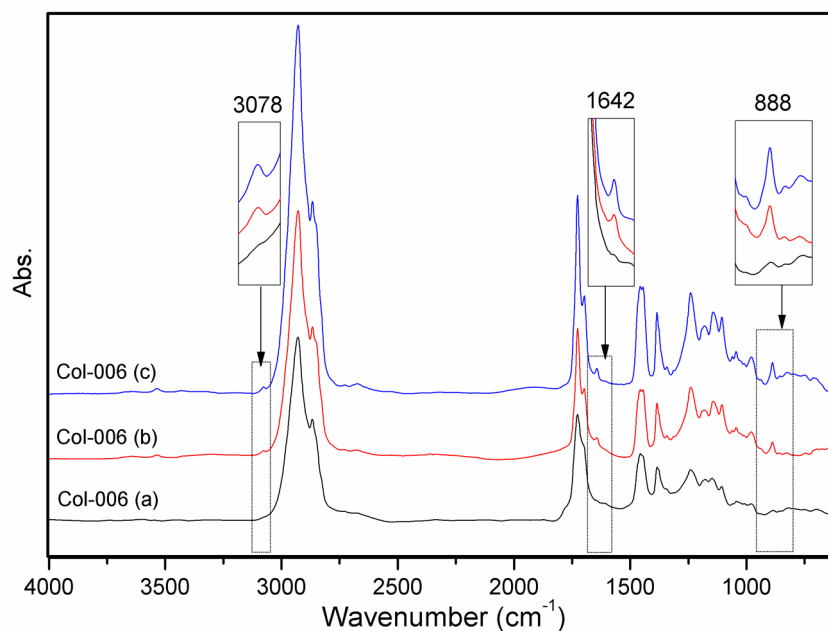


**Figure 7.** IR spectra of sample Col-006 after multi-stage heat–pressure treatment at different depths from the surface. With increasing sampling depth (a–c), the bands at 3078, 1642 and 888  $\text{cm}^{-1}$  began to reappear with increasing intensity.

### 3.2. Borneo Copal Resin

#### 3.2.1. FTIR Spectroscopy

According to previous studies [3,17,18], the spectroscopic characteristics of Borneo copal resins (Figure 8) include four absorption peaks caused by C–H stretching near 2957, 2930, 2870 and 2850  $\text{cm}^{-1}$ , with one strong peak at 1710  $\text{cm}^{-1}$  and one shoulder peak at 1733  $\text{cm}^{-1}$  assigned to C=O stretching. Features at 1464, 1384 and 1368  $\text{cm}^{-1}$  are due to  $\text{CH}_2\text{--CH}_3$  bending vibration, and 1253, 1165 and 1044  $\text{cm}^{-1}$  peaks to C–O stretching vibration. The spectra also contain IR absorption peaks near 973 and 888  $\text{cm}^{-1}$ , assigned to C–H bending vibration.

Compared with ambers, the IR absorption peaks of Borneo copal resin due to C=O stretching, near 1733 and 1710  $\text{cm}^{-1}$ , are distinctly weak. The peak near 1165  $\text{cm}^{-1}$ , attributed to C–O stretching, is extremely weak, indicating a low degree of esterification and low concentrations of C=O and C–O, which are generally considered to be related to ester and ketone groups in copal resins and ambers [29].

Compared with Colombia and Madagascar copal resins, IR spectra of Borneo samples have different main absorption peaks and lack bands at 3078 and 1642  $\text{cm}^{-1}$ , but still have a weak feature at 888  $\text{cm}^{-1}$ .

IR characteristics before and after treatment are shown in Table 6.

The ratio of peak heights at 1710 and 1464  $\text{cm}^{-1}$ ,  $H^{1710}/H^{1464}$ , in the IR spectra seems to be related to resin maturity, as is the  $H^{1710}/H^{2957}$  ratio. Before treatment, the  $H^{1710}/H^{1464}$  ratio of Borneo copal resins was 0.24–0.40, and the  $H^{1710}/H^{2957}$  ratio 0.06–0.10.

After the slow low-temperature (e.g., Bor-002, Figure 8a) and rapid high-temperature treatments (e.g., Bor-026, Figure 8b), the  $H^{1710}/H^{1464}$  ratio increased to 0.45–1.29 and the ratio  $H^{1710}/H^{2957}$  ratio to 0.12–0.47.

After other three heat–pressure experiments (e.g., Bor-004, 011, 010, Figure 8c–e), spectral changes were similar to those recorded in the two heat treatments, with the ratios  $H^{1710}/H^{1464}$  and  $H^{1710}/H^{2957}$  increasing to 0.50–0.73 and 0.14–0.20, respectively.

These results indicate that the IR absorption bands attributed to C=O stretching at 1733–1710  $\text{cm}^{-1}$  and C–O stretching at 1175–1165  $\text{cm}^{-1}$  became stronger with increasing concentrations of C=O and C–O. These modification methods are thus able to accelerate the maturation of Borneo copal resins.

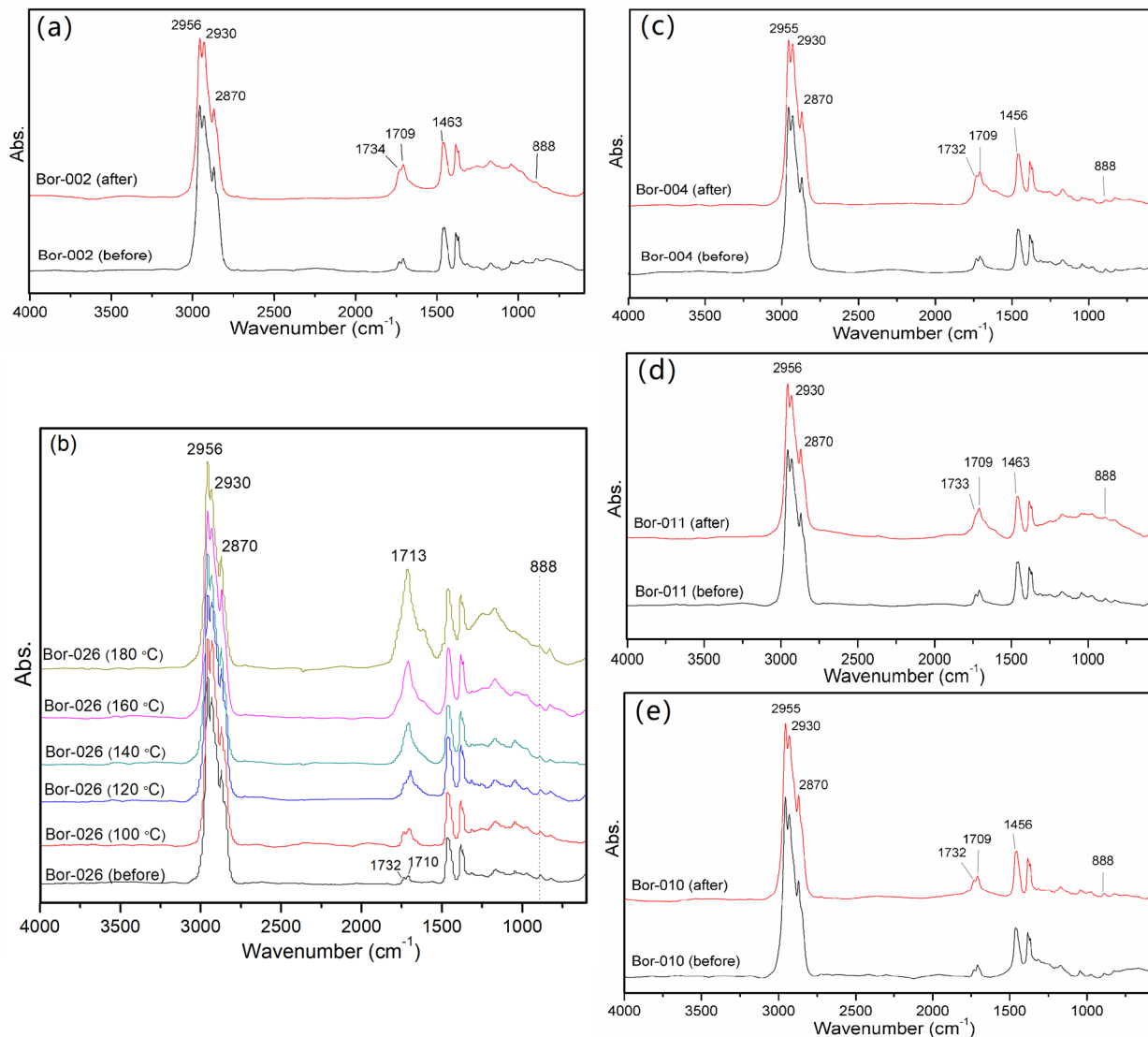


**Figure 8.** IR spectra of Borneo samples before and after treatment: (a) slow low-temperature treatment; (b) rapid high-temperature treatment; (c) single-stage heat–pressure treatment (140/25); (d) single-stage heat–pressure treatment (180/35); (e) multi-stage heat–pressure treatment.

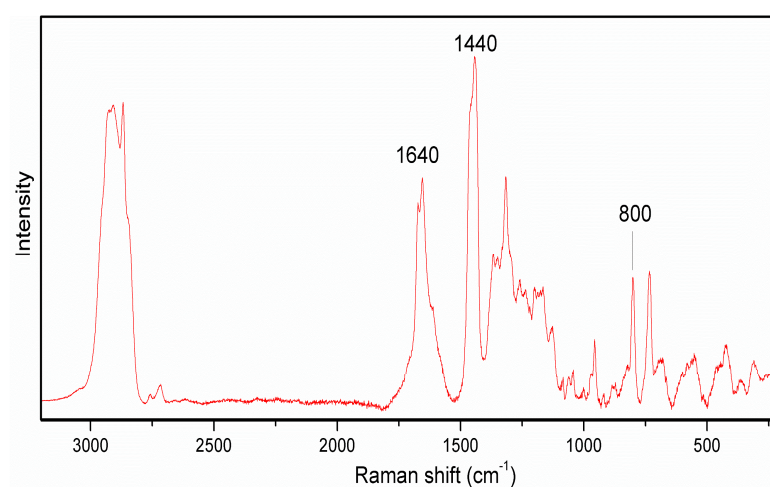
### 3.2.2. Raman Spectroscopy

Raman spectra of copal resins from Borneo differed from those of the Colombia and Madagascar copal resins with a lack of a peak at  $1200\text{ cm}^{-1}$ , usually assigned to  $\delta(\text{CCH})$  modes of terpenoids or  $\delta(\text{C-O})$  modes. The extra feature at  $800\text{ cm}^{-1}$  occurs only in the spectra of Borneo copal resins (Figure 9) and was attributed to aromatic hydrocarbon deformations in previous studies, explaining the characteristic strong luminescence of these resins [22,23,30]. Raman spectral profiles are also related to the botanical sources, as Borneo resins are from the *Dipterocarpaceae* family and Colombia and Madagascar resins from *Hymenaea* species.

In contrast to the Colombia and Madagascar copal resins, it was difficult to acquire high-quality Raman spectra of Borneo samples due to their strong fluorescence background and weak peaks near  $2700\text{--}3100$ ,  $1640$  and  $1440\text{ cm}^{-1}$ . After heat treatment, the fluorescence backgrounds became stronger and the peaks less obvious or obscured by the background. It is therefore difficult to confirm alterations of maturities of Borneo samples during treatment based on  $\text{H}^{1640}/\text{H}^{1440}$  ratios.

**Table 6.** Changes in IR spectra of Borneo copal resins during treatment.

Sample	Modification Methods	Changes in Infrared Spectra				
		Before Treatment		After Treatment		
		H <sup>1710</sup> /H <sup>1464</sup>	H <sup>1710</sup> /H <sup>2957</sup>	H <sup>1710</sup> /H <sup>1464</sup>	H <sup>1710</sup> /H <sup>2957</sup>	
Bor-002	Slow low-temperature treatment	0.28	0.08	0.61	0.21	
Bor-026	Rapid high-temperature treatment	0.24	0.06	100 °C	0.45	0.12
				120 °C	0.46	0.15
				140 °C	0.70	0.20
				160 °C	0.78	0.25
				180 °C	1.29	0.47
Bor-004	Single-stage heat-pressure treatment (140/25)	0.41	0.11	0.50	0.17	
Bor-011	Single-stage heat-pressure treatment (180/35)	0.40	0.10	0.73	0.20	
Bor-010	Multi-stage heat-pressure treatment	0.37	0.09	0.51	0.14	

**Figure 9.** Raman spectrum of Borneo copal resin (fluorescence background subtracted).

### 3.2.3. NMR Spectroscopy

The single-bond region of <sup>13</sup>C NMR spectra of Borneo copal resins is dominated by five peaks at 16, 22, 27, 37 and 48 ppm, with all assigned to saturated carbons. The only other significant resonances are two broad peaks at 126 and 134 ppm in the alkene region, as found in straight chains or rings [31]. The <sup>13</sup>C spectra lack resonances in the carbonyl region at 160–220 ppm, with ketones, aldehydes, esters and carboxylic acids being either absent or below detectable thresholds. The spectra also lack resonances of C=C double bonds of terminal-chain and unsubstituted-exocyclic alkenes at 107 ppm, and fully substituted double bonds at 148 ppm, indicating that the content of unsaturated terpene components is relatively low in Borneo copal resin, consistent with their IR spectra.

The <sup>13</sup>C NMR spectra of the Borneo copal resin samples did not change significantly during the modification treatments (Figure 5b).

### 3.2.4. Comparison of Copal and Amber Spectra

Comparison of IR spectra of Borneo copal resins treated with five modification conditions indicates that the effects of three heat-pressure experiments are not ideal. Sample melting was obvious, but with no apparent changes in IR spectra. Relatively speaking, the slow low-temperature treatment is more practicable than the other methods. The sample did not change significantly in appearance after treatment, while in the IR spectrum, peaks at  $1733\text{--}1710\text{ cm}^{-1}$  assigned to C=O stretching and at  $1175\text{--}1165\text{ cm}^{-1}$  due to C–O stretching were obviously enhanced, indicating that the concentration of these groups increased, and similarities with IR spectra of heat-treated ambers from deposits around the Baltic Sea were also enhanced.

For heat-treated Baltic ambers, increases in temperature and heating time resulted in the IR C=O stretching band at around  $1735\text{ cm}^{-1}$  shifting to a lower wavenumber, as low as around  $1710\text{ cm}^{-1}$ , while C–O stretching vibration at  $1157\text{ cm}^{-1}$  shifted to a higher wavenumber, reaching  $1175\text{ cm}^{-1}$ . The intensity of the broad absorption shoulder attributed to C–O stretching in the range of  $1250\text{--}1175\text{ cm}^{-1}$  was greatly enhanced. In addition, previous studies [11,18,32] considered that this shoulder (the “Baltic shoulder”) at  $1250\text{--}1175\text{ cm}^{-1}$  is related to the presence of succinic acid and its esters in amber samples from that region and is a characteristic of significance in identifying origins.

When the Borneo copal resin samples were heated to  $180\text{ }^{\circ}\text{C}$  in the rapid high-temperature method, the double peaks of sample Bor-026 at  $1733$  and  $1710\text{ cm}^{-1}$  merged into a strong absorption band at  $1717\text{ cm}^{-1}$ , and the peak near  $1165\text{ cm}^{-1}$  was enhanced and shifted to a higher wavenumber, forming a broad absorption shoulder similar to the Baltic shoulder at  $1250\text{--}1175\text{ cm}^{-1}$ , which means samples could be confused with Baltic amber (Figure 10). The main difference between the two IR spectra is the absence of a peak near  $2957\text{ cm}^{-1}$  assigned to C–H stretching in the IR spectra of Baltic ambers.

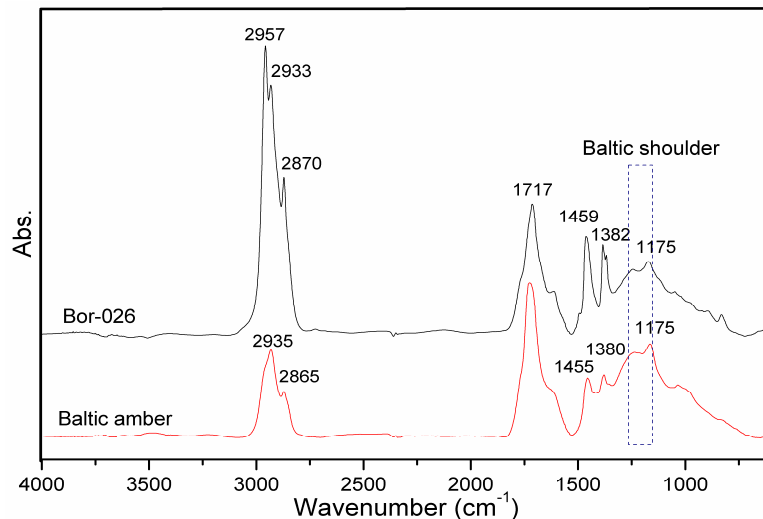


**Figure 10.** IR spectra of heat-treated Baltic amber and sample Bor-026 after rapid high-temperature treatment at  $180\text{ }^{\circ}\text{C}$ .

## 4. Conclusions

The two types of copal resin studied here were thought to be completely different and could be easily distinguished from ambers before they were modified by heat and/or pressure treatment. However, their maturities are supposed to be significantly enhanced by proper treatment, with their appearance and spectral characteristics then being very similar to those of ambers.

We designed five methods for modifying the copal resins, through which their color darkened and similarities to ambers were enhanced. However, analyses by FTIR, Raman and  $^{13}\text{C}$  NMR spectroscopy were able to detect the changes.

Multi-stage heat–pressure treatment was most effective for copal resins from Colombia and Madagascar, with IR spectral features at 3078, 1642, 888  $\text{cm}^{-1}$  being greatly reduced, with their spectra then being similar to those of Dominican and Mexican ambers. The change in peak height ratio near 1640 and 1440  $\text{cm}^{-1}$  ( $\text{H}^{1640}/\text{H}^{1440}$ ) in Raman spectra can be used as an indicator of treatment effect, whereas NMR resonance peaks at 107 and 148 ppm were obviously weakened after treatment. However, these modification methods cannot replace tens of millions of years of geological processes and any changes in appearance and spectral characteristics are limited to the surface and near-surface, with sample interiors maintaining original resin features.

For copal resins from Borneo, the slow low-temperature treatment method was more effective, with the resemblance to IR spectra of ambers being enhanced. Disregarding the damage to samples, when Borneo copal resins were heated at 180 °C in the rapid high-temperature method, their IR spectra were similar to that of heat-treated Baltic amber to some extent, including the “Baltic shoulder” at 1250–1175  $\text{cm}^{-1}$ ; the main difference was the lack of a band near 2957  $\text{cm}^{-1}$  in the amber spectra.

**Author Contributions:** Formal analysis, T.L.; funding acquisition, H.L.; methodology, H.L., T.L. and T.Z.; project administration, H.L.; investigation, X.C., B.L. and Y.L.; supervision, T.L.; writing—original draft preparation, T.Z.; writing—review and editing, H.L. and T.L. All authors have read and agreed to the published version of the manuscript.

**Funding:** This research was funded by NGTC Scientific Research Fund Project No. NGTC2019009 “Study on Identification of Ambers’ Origin” and No. NGTCQT18005 “The Research on Identification of Heat-Pressurized Copal Resins and Ambers”.

**Institutional Review Board Statement:** Not Applicable.

**Informed Consent Statement:** Not Applicable.

**Acknowledgments:** We thank Peng Dou, Liang Chen, Chun Min Yu, Jun Tan, Zhen Xi Xiong and Gui Shan Xu for their assistance in the course of the study.

**Conflicts of Interest:** The authors declare no conflict of interest.

## References

1. Abduriyim, A.; Kimura, H.; Yokoyama, Y.; Nakazono, H.; Wakatsuki, M.; Shimizu, T.; Tansho, M.; Ohki, S. Characterization of “Green Amber” with Infrared and Nuclear Magnetic Resonance Spectroscopy. *Gems Gemol.* **2009**, *45*, 158–177. [CrossRef]
2. Qi, L.; Yuan, X.; Chen, M.; Lin, S. ESR Behavior and  $^{13}\text{C}$  NMR Representation of Treated Amber and Resin. *J. Gems Gemmol.* **2003**, *2*. Available online: [https://en.cnki.com.cn/Article\\_en/CJFDTotal-BSHB200302000.htm](https://en.cnki.com.cn/Article_en/CJFDTotal-BSHB200302000.htm) (accessed on 6 September 2021).
3. Qi, L.; Zhou, Z.; Liao, G.; Xiong, Z. Polymerization Behavior and  $^{13}\text{C}$  NMR Representation of Green Copal Resins under Heat-Pressurized Process. *J. Gems Gemmol.* **2010**, *12*, 9–13.
4. Stach, P.; Martinkutė, G.; Šinkūnas, P.; Natkaniec-Nowak, L.; Drzewicz, P.; Naglik, B.; Bogdasarov, M. An Attempt to Correlate the Physical Properties of Fossil and Subfossil Resins with Their Age and Geographic Location. *J. Polym. Eng.* **2019**, *39*, 716–728. [CrossRef]
5. Montoro, Ó.; Lobato, Á.; Garcia Baonza, V.; Taravillo, M. Infrared Spectroscopic Study of the Formation of Fossil Resin Analogs with Temperature Using Trans -Communic Acid as Precursor. *Microchem. J.* **2018**, *141*, 294–300. [CrossRef]
6. Kimura, H.; Tsukada, Y.; Mita, H.; Yamamoto, Y.; Chujo, R.; Yukawa, T. A Spectroscopic Index for Estimating the Age of Amber. *Bull. Chem. Soc. Jpn.* **2006**, *79*, 451–453. [CrossRef]
7. Solórzano Kraemer, M.M.; Delclòs, X.; Engel, M.; Peñalver, E. A Revised Definition for Copal and Its Significance for Palaeontological and Anthropocene Biodiversity-Loss Studies. *Sci. Rep.* **2020**, *10*, 19904. [CrossRef]
8. Kocsis, L.; Usman, A.; Jourdan, A.-L.; Hassan, S.; Jumat, N.; Daud, D.; Briguglio, A.; Slik, F.; Rinyu, L.; Futó, I. The Bruneian Record of “Borneo Amber”: A Regional Review of Fossil Tree Resins in the Indo-Australian Archipelago. *Earth-Sci. Rev.* **2019**, *201*, 103005. [CrossRef]
9. Delclòs, X.; Peñalver, E.; Ranaivosoa, V.; Solórzano Kraemer, M.M. Unravelling the Mystery of “Madagascar Copal”: Age, Origin and Preservation of a Recent Resin. *PLoS ONE* **2020**, *15*, e0232623. [CrossRef]
10. Wang, Y.; Yang, Y.; Yang, M. Experimental Study on Enhancement Technique of Amber. *J. Gems Gemmol.* **2010**, *46*, 218–240.
11. Wang, Y.; Yang, M.; Yang, Y.; Niu, P. Critical Evidences for Identification of Heated Ambers. *J. Gems Gemmol.* **2010**, *4*. Available online: [https://en.cnki.com.cn/Article\\_en/CJFDTotal-BSHB201004009.htm](https://en.cnki.com.cn/Article_en/CJFDTotal-BSHB201004009.htm) (accessed on 6 September 2021).
12. Lambert, J.; Nguyen, T.; Levy, A.; Wu, Y.; Santiago-Blay, J. Structural Changes from Heating Amber and Copal as Observed by Nuclear Magnetic Resonance Spectroscopy. *Magn. Reson. Chem.* **2020**, *58*. [CrossRef]



13. Anderson, K.; Winans, R.; Botto, R.E. The Nature and Fate of Natural Resins in the Geosphere—II. Identification, Classification and Nomenclature of Resinites. *Org. Geochem.* **1992**, *18*, 829–841. [[CrossRef](#)]
14. McCoy, V.; Boom, A.; Solórzano Kraemer, M.M.; Gabbott, S. The Chemistry of American and African Amber, Copal, and Resin from the Genus Hymenaea. *Org. Geochem.* **2017**, *113*, 43–54. [[CrossRef](#)]
15. Lambert, J.; Santiago-Blay, J.; Wu, Y.; Levy, A. Examination of Amber and Related Materials by NMR Spectroscopy. *Magn. Reson. Chem.* **2015**, *53*, 2–8. [[CrossRef](#)]
16. Langenheim, J.H. *Plant Resins: Chemistry, Evolution, Ecology, and Ethnobotany*; Timber Press: Portland, OR, USA, 2003; ISBN 0-88192-574-8.
17. Dai, L.; Shi, G.; Yuan, Y.; Wang, M.; Wang, Y. Infrared Spectroscopic Characteristics of Borneo and Madagascar Copal Resins and Rapid Identification between Them and Ambers with Similar Appearances. *Spectrosc. Spectr. Anal.* **2018**, *38*, 2123–2131.
18. Brody, R.; Edwards, H.; Pollard, A. A Study of Amber and Copal Samples Using FT-Raman Spectroscopy. *Spectrochim. Acta A Mol. Biomol. Spectrosc.* **2001**, *57*, 1325–1338. [[CrossRef](#)]
19. Guiliano, M.; Asia, L.; Onoratini, G.; Mille, G. Applications of Diamond Crystal ATR FTIR Spectroscopy to the Characterization of Ambers. *Spectrochim. Acta A Mol. Biomol. Spectrosc.* **2007**, *67*, 1407–1411. [[CrossRef](#)]
20. Edwards, H.; Farwell, D.; Jorge-Villar, S. Raman Microspectroscopic Studies of Amber Resins with Insect Inclusions. *Spectrochim. Acta A Mol. Biomol. Spectrosc.* **2008**, *68*, 1089–1095. [[CrossRef](#)] [[PubMed](#)]
21. Winkler, W.; Kirchner, E.; Asenbaum, A.; Musso, M. A Raman Spectroscopic Approach to the Maturation Process of Fossil Resins. *J. Raman Spectrosc.* **2001**, *32*, 59–63. [[CrossRef](#)]
22. Vandenabeele, P.; Grimaldi, D.; Edwards, H.; Moens, L. Raman Spectroscopy of Different Types of Mexican Copal Resins. *Spectrochim. Acta A Mol. Biomol. Spectrosc.* **2003**, *59*, 2221–2229. [[CrossRef](#)]
23. Naglik, B.; Mroczkowska-Szerszeń, M.; Dumanska-Słowik, M.; Natkaniec-Nowak, L.; Drzewicz, P.; Stach, P.; Żukowska, G. Fossil Resins—Constraints from Portable and Laboratory Near-Infrared Raman Spectrometers. *Minerals* **2020**, *10*, 104. [[CrossRef](#)]
24. Montoro, O.; Taravillo, M.; Moya, M.; Roja, J.; Barrero, A.; Arteaga, P.; Garcia Baonza, V. Raman Spectroscopic Study of the Formation of Fossil Resin Analogues. *J. Raman Spectrosc.* **2014**, *45*, 1230–1235. [[CrossRef](#)]
25. Xing, Y.; Qi, L.; Mai, Y.; Xie, M. FTIR and  $\delta^{13}\text{C}$  NMR Spectrum Characterization and Significance of Amber from Different Origins. *J. Gems Gemmol.* **2015**, *17*, 8–16.
26. Lambert, J.; Frye, J. Carbon Functionalities in Amber. *Science* **1982**, *217*, 55–57. [[CrossRef](#)] [[PubMed](#)]
27. Lambert, J.; Frye, J.; Poinar, G. Analysis of North American Amber by Carbon-13 NMR Spectroscopy. *Geoarchaeology* **1990**, *5*, 43–52. [[CrossRef](#)]
28. Lambert, J.; Frye, J.; Poinar, G. Amber from the Dominican Republic: Analysis by Nuclear Magnetic Resonance Spectroscopy. *Archaeometry* **1985**, *27*, 43–51. [[CrossRef](#)]
29. Park, J.; Yun, E.Y.; Kang, H.; Ahn, J.; Kim, G. IR and Py/GC/MS Examination of Amber Relics Excavated from 6th Century Royal Tomb in Korean Peninsula. *Spectrochim. Acta A Mol. Biomol. Spectrosc.* **2016**, *165*, 114–119. [[CrossRef](#)] [[PubMed](#)]
30. Jehlička, J.; Jorge-Villar, S.; Edwards, H. Fourier Transform Raman Spectra of Czech and Moravian Fossil Resins from Freshwater Sediments. *J. Raman Spectrosc.* **2004**, *35*, 761–767. [[CrossRef](#)]
31. Lambert, J.; Levy, A.; Santiago-Blay, J.; Wu, Y. Nuclear Magnetic Resonance Characterization of Indonesian Amber. *Life Excit. Biol.* **2013**, *1*, 136–155. [[CrossRef](#)]
32. Yang, Y.; Wang, Y. Summary on Organic Components and Relevant Spectral Characteristics of Amber and Copal. *J. Gems Gemmol.* **2010**, *12*, 16–22.